Status of the Cabibbo-Kobayashi-Maskawa matrix and Unitarity Triangle fits

M. Bona, M. Ciuchini, E. Franco, V. Lubicz, G. Martinelli, F. Parodi, M. Pierini, P. Roudeau, C. Schiavi, L. Silvestrini, et al.

Status of the Cabibbo-Kobayashi-Maskawa matrix and Unitarity Triangle fits

M. Bona[*], M. Ciuchini[†], E. Franco[**], V. Lubicz[‡], G. Martinelli[**], F. Parodi[§], M. Pierini[¶], P. Roudeau[‖], C. Schiavi[§], L. Silvestrini[**], V. Sordini[‖], A. Stocchi[‖] and V. Vagnoni[††]

[*]*Lab. d'Annecy-le-Vieux de Physique des Particules LAPP, IN2P3/CNRS, Université de Savoie*
[†]*Dip. di Fisica, Università di Roma Tre and INFN, Sez. di Roma III, Roma, Italy*
[**]*Dip. di Fisica, Università di Roma "La Sapienza" and INFN, Sez. di Roma, Roma, Italy*
[‡]*Dip. di Fisica, Università di Roma Tre and INFN, Sez. di Roma III, I-00146 Roma, Italy*
[§]*Dip. di Fisica, Università di Genova and INFN, Genova, Italy*
[¶]*Department of Physics, University of Wisconsin, Madison, USA*
[‖]*Lab. de l'Accélérateur Linéaire, IN2P3-CNRS et Univ. de Paris-Sud, Orsay Cedex, France*
[††]*Corresponding author, INFN, Sez. di Bologna, Bologna, Italy*

Abstract. The status of the Unitarity Triangle analysis realized by the **UT***fit* Collaboration is presented. The most recent determinations of theoretical and experimental parameters are used in order to over-constrain the apex of the Unitarity Triangle in the Standard Model. In addition, we present the analysis of the Unitarity Triangle beyond the Standard Model, by parametrizing New Physics contributions in $\Delta F = 2$ processes. With the new measurements from the Tevatron, namely the mass difference Δm_s, the width difference $\Delta\Gamma_s$ and the di-muon asymmetry, it is possible to establish significant bounds on New Physics parameters also in the B_s sector. The results and the plots presented in this paper can be found at the URL `http://www.utfit.org`, where they are continuously kept up-to-date.

Keywords: Cabibbo-Kobayashi-Maskawa matrix, Unitarity Triangle, New Physics
PACS: 13.25.Hw, 12.15.Hh

INTRODUCTION

The analysis of the Unitarity Triangle (UT) and CP violation represents at the moment one of the key places where the Standard Model (SM) can be tested with outstanding precision, hence it provides a great opportunity to search and discover New Physics (NP) effects beyond the SM. During the recent years an unprecedented amount of new measurements, thanks to the successes of the B factories and the Tevatron, has been made available to the UT analysis, allowing for a precise determination of the parameters of the Cabibbo-Kobayashi-Maskawa (CKM) matrix.

The measurements used in the Standard Model UT analysis include the sides of the UT, namely $|V_{ub}|/|V_{cb}|$ from semileptonic decays, and the magnitudes of the mixing amplitudes of the neutral B mesons Δm_d and Δm_s, as well as ε_K, which parametrizes the indirect CP violation in the neutral Kaon system. Besides these quantities, which require the employment of non-perturbative hadronic parameters coming from lattice computations in order to be obtained, as in the case of $|V_{ub}|/|V_{cb}|$, or related to the CKM factors $\bar{\rho}$ and $\bar{\eta}$ in the other cases, several determinations of the UT angles α, β and γ

not requiring aid from the lattice are available.

Such an abundance of measurements, which can be basically unaffected from NP as in the case of $|V_{ub}|/|V_{cb}|$ and of the tree-level determination of γ from $B \to D^{(*)} K^{(*)}$, or alternatively affected by the presence of NP contributions in different ways, allows for a simultaneous determination of SM and NP parameters in the flavour sector. As it will be shown, the UT analysis in the presence of NP has reached nowadays an accuracy comparable to the SM analysis, thus providing very stringent constraints on NP contributions to $\Delta F = 2$ processes.

The **UT***fit* Collaboration has already published a series of papers, where the interested reader can find all the details not reported in this brief document [1, 2, 3, 4].

In the following we will show first the results of the SM analysis, i.e. assuming the validity of the SM. Then, upon the introduction of a generalized parametrization of $\Delta F = 2$ processes, we will discuss the UT fit in the presence of NP, thus showing the bounds so obtained on NP quantities. By restricting the NP scenario to Minimal Flavour Violation (MFV) models, both in the large and small $\tan\beta$ regimes, we will estimate the corresponding NP scales which are probed by means of the currently available experimental information.

STANDARD MODEL ANALYSIS

Before the advent of the B factories, UT fits were performed by only using measurements of the sides and indirect CP violation in neutral Kaon system. Several determinations of UT angles, thanks to the results coming from the B factories, allowed for a dramatical improvement of our knowledge of the UT.

Several measurements at present bound the range of the $\bar{\rho}$ and $\bar{\eta}$ parameters. Here below a brief description of the most relevant ones in use in our UT fit is reported:

- The rates of charmed and charmless semileptonic B decays decays which allow to measure the ratio $|V_{ub}|/|V_{cb}|$.
- The mass difference between the light and heavy mass eigenstates of the $B_d^0 - \bar{B}_d^0$ system Δm_d.
- The mass difference of the $B_s^0 - \bar{B}_s^0$ system Δm_s, compared to Δm_d, $\Delta m_d/\Delta m_s$.
- The ε_K parameter, which measures CP violation in the neutral kaon system.
- $\sin 2\beta$ from the golden modes $B_d^0 \to c\bar{c}K^0$, that can be determined almost without hadronic uncertainties.
- The angle α, that can be obtained from the $B \to \pi\pi$ and $B \to \rho\rho$ decays, assuming the SU(2) flavour symmetry and neglecting the contributions of electroweak penguins. It can also be obtained using a time-dependent analysis of $B \to (\rho\pi)^0$ decays on the Dalitz plane. Fig. 1 shows the combination of the BaBar and Belle results including all the three methods, as well as and the bound on the $\bar{\rho} - \bar{\eta}$ plane. We obtain:

$$\alpha = ([7,\ 9]^\circ \cup [80,\ 107]^\circ \cup [159,\ 177]^\circ\ @95\%) \tag{1}$$

  The multimodal shape of the α p.d.f. is due to the intrinsic ambiguities of the methods used for its determination. The SM solution corresponds to the central

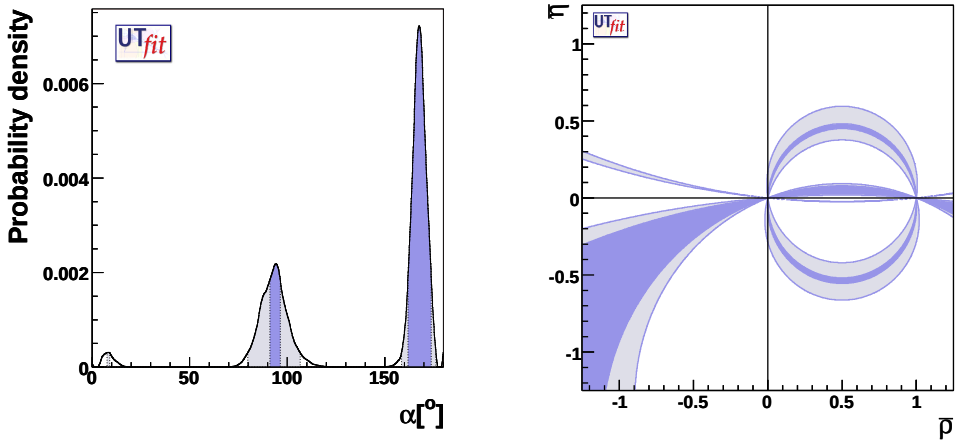

FIGURE 1. Left plot: p.d.f. for α resulting from the combination of the BaBar and Belle results. Right plot: corresponding bound on the $\bar{\rho}-\bar{\eta}$ plane, 68% and 95% confidence regions.

peak, and just considering it (e.g., using other constraints to discard the non-SM solutions) we get $\alpha = (92 \pm 7)^\circ$.

- The angle γ that can be extracted from the tree-level decays $B \to DK$, using the fact that a charged B can decay into a $D^0(\overline{D}^0)K$ final state via a $V_{cb}(V_{ub})$ mediated process. CP violation occurs if the D^0 and the $\overline{D}^0$ decay to the same final state. The same argument can be applied to $B \to D^*K$ and $B \to D^{(*)}K^*$ decays. Three methods have been proposed:
  - The Gronau-London-Wyler method (GLW). It consists in reconstructing the neutral D meson in a CP eigenstate: $B^\pm \to D^0_{CP^\pm}K^\pm$, where $D^0_{CP^\pm}$ are the CP eigenstates of the D meson.
  - The Atwood-Dunietz-Soni method (ADS). It consists in forcing the $\bar{D}^0$ (D^0) meson, coming from the Cabibbo-suppressed (Cabibbo-allowed) $b \to u$ ($b \to c$) transition to decay into the Cabibbo-allowed (Cabibbo-suppressed) $K\pi$ final state. In this way, one can look at the interference between two amplitudes.
  - Dalitz method. It consists in studying the interference between the $b \to u$ and the $b \to c$ transitions using the Dalitz plot of D mesons reconstructed into three-body final states (such as $D^0 \to K_s\pi^-\pi^+$). The advantage of this method is that the full sub-resonance structure of the three-body decay is considered, including interferences such as those used for GLW and ADS methods plus additional interferences due to the overlap between broad resonances in some regions of the Dalitz plot.

Fig. 2 shows the combination of the BaBar and Belle results including all the three methods, as well as and the bound on the $\bar{\rho}-\bar{\eta}$ plane.
We obtain:

$$\gamma = (78 \pm 30)^\circ \cup (-102 \pm 30)^\circ \tag{2}$$

As in the case of the α angle, the p.d.f. for γ is multimodal due to a remaining two-fold ambiguity.

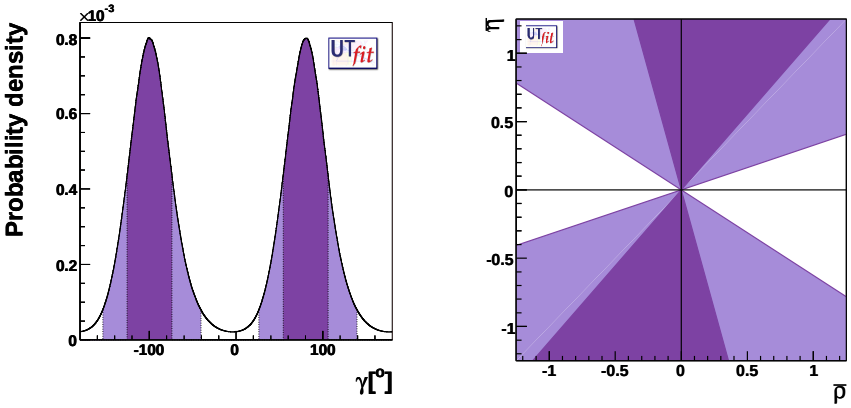

FIGURE 2. Left plot: p.d.f. for γ resulting from the combination of the BaBar and Belle results. Right plot: corresponding bound on the $\bar{\rho} - \bar{\eta}$ plane, 68% and 95% confidence regions.

TABLE 1. Values of the relevant input quantities used in the UT fit. The Gaussian and the flat contributions to the uncertainty are given in the third and fourth columns respectively (for details on the statistical treatment see [5]).

Parameter	Value	Gaussian (σ)	Uniform (half-width)
λ	0.2258	0.0014	-
$\lvert V_{cb}\rvert$(excl.)	41.3×10^{-3}	1.0×10^{-3}	1.8×10^{-3}
$\lvert V_{cb}\rvert$(incl.)	41.6×10^{-3}	0.7×10^{-3}	-
$\lvert V_{ub}\rvert$(excl.)	35.0×10^{-4}	4.0×10^{-4}	-
$\lvert V_{ub}\rvert$(incl.)	44.9×10^{-4}	3.3×10^{-4}	-
Δm_d	0.507 ps^{-1}	0.005 ps^{-1}	-
Δm_s	17.33 ps^{-1}	$^{+0.33}_{-0.18} \pm 0.07$ ps^{-1}	-
$f_{B_s}\sqrt{\hat{B}_{B_s}}$	262 MeV	35 MeV	-
$\xi = \frac{f_{B_s}\sqrt{\hat{B}_{B_s}}}{f_{B_d}\sqrt{\hat{B}_{B_d}}}$	1.23	0.06	-
$\hat{B}_K$	0.79	0.04	0.08
ε_K	2.280×10^{-3}	0.013×10^{-3}	-
f_K	0.160 GeV	fixed	
Δm_K	0.5301×10^{-2} ps^{-1}	fixed	
$\sin 2\beta$	0.675	0.026	-
$\overline{m}_t$	163.8 GeV	3.2 GeV	-
$\overline{m}_b$	4.21 GeV	0.08 GeV	-
$\overline{m}_c$	1.3 GeV	0.1 GeV	-
$\alpha_s(M_Z)$	0.119	0.003	-

In Tab. 1 we summarize the values of the relevant input parameters used in the fit.

TABLE 2. Determination of UT parameters from the SM fit.

Parameter	Output	Parameter	Output
$\overline{\rho}$	0.162 ± 0.029	$\overline{\eta}$	0.342 ± 0.017
$\alpha[^\circ]$	92.9 ± 4.4	$\beta[^\circ]$	22.1 ± 0.9
$\gamma[^\circ]$	64.6 ± 4.4	Δm_s [ps^{-1}]	17.4 ± 0.3
$\sin 2\beta$	0.698 ± 0.023	Imλ_t [10^{-5}]	13.7 ± 0.6
$V_{ub}[10^{-3}]$	3.67 ± 0.15	$V_{cb}[10^{-2}]$	4.16 ± 0.06
$V_{td}[10^{-3}]$	8.51 ± 0.28	$\lvert V_{td}/V_{ts}\rvert$	0.208 ± 0.007
R_b	0.379 ± 0.015	R_t	0.904 ± 0.030

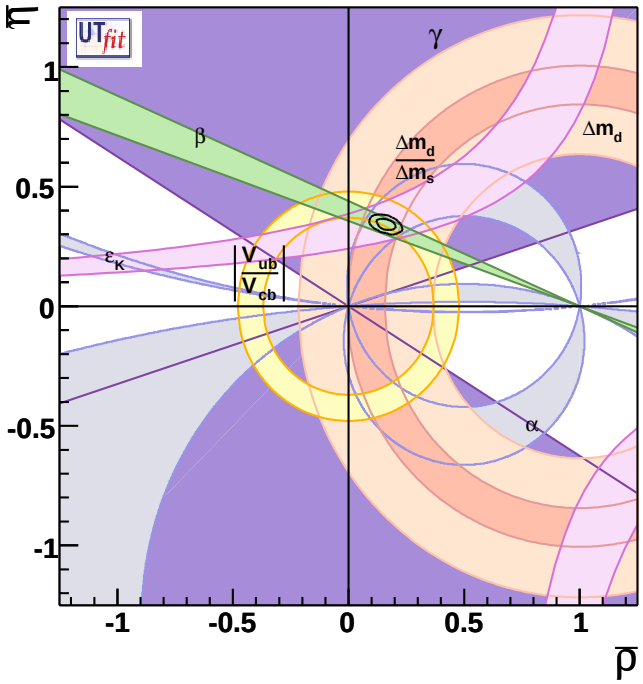

FIGURE 3. Determination of $\bar{\rho}$ and $\bar{\eta}$ from constraints on $|V_{ub}|/|V_{cb}|$, Δm_d, Δm_s, ε_K, β, γ, and α. 68% and 95% total probability contours are shown, together with 95% probability regions from the individual constraints.

The output of the SM fit including all the constraints is reported in Tab. 2 and in Fig. 3. By looking in more detail at Fig. 3, it is interesting to note that the 95% confidence regions depicted by the $\sin 2\beta$ and $|V_{ub}|/|V_{cb}|$ constraints, being them two of the most precise ones used in the fit, show just a bare agreement. In particular, in our analysis we find that while the experimental value of $\sin 2\beta$ is in good agreement with the rest of the fit, the same does not hold for $|V_{ub}|/|V_{cb}|$, which is rather on the higher side. It

can be shown that this is due to a large value of the inclusive determination of $|V_{ub}|$. Unless this discrepancy should be considered as a hint of NP, it has to be explained by the uncertainties of the theoretical approaches. It is worth recalling that the value of $|V_{ub}|$ that is extracted from the experiments also relies on non perturbative hadronic quantities.

Nevertheless, it should be remarked that the UT analysis has shown so far an impressive success of the CKM picture in describing CP violation in the SM.

NEW PHYSICS ANALYSIS

Starting from a tree-level determination of $\bar{\rho}$ and $\bar{\eta}$, we perform the UT analysis in general extensions of the SM with arbitrary NP contributions to $|\Delta F| = 2$ processes. We will show that the recent measurements from B factories and the Tevatron allow us to determine with good precision the shape of the UT even in the presence of NP, and to draw significant bounds on NP contributions to $|\Delta F| = 2$ processes.

In particular, three results have dramatically improved the knowledge of the UT beyond the SM, extending our view in the B_s sector. First, the measurement of Δm_s from CDF [6], which reduces the uncertainty of the SM fit and has a strong impact on the determination of the Universal Unitarity Triangle (UUT) [7] in models with Minimal Flavour Violation (MFV) [8, 9, 10, 11, 12, 13, 14]. Moreover, it allows for the first time to put a bound on NP corrections to the magnitude of the B_s mixing amplitude. As far as the B_s mixing phase is concerned, useful information to put relevant bounds can be extracted from the measurement of the dimuon asymmetry in $p\bar{p}$ collisions by the D0 experiment [15] and of the B_s width difference.

We assume that NP enters observables in the flavour sector only at the loop level. For this reason the constraints from V_{ub}/V_{cb} and γ from the interference between $b \to c$ and $b \to u$ transitions to DK final states are basically NP-free. Being the mixing processes described by a single amplitude, they can be parameterized without loss of generality in terms of two parameters quantifying the difference of the amplitude with respect to the SM one [16, 17, 18, 19, 20]. In the case of $B_q^0 - \bar{B}_q^0$ mixing we define

$$C_{B_q} e^{2i\phi_{B_q}} = \frac{\langle B_q^0 | H_{\rm eff}^{\rm full} | \bar{B}_q^0 \rangle}{\langle B_q^0 | H_{\rm eff}^{\rm SM} | \bar{B}_q^0 \rangle}, \qquad (q = d, s) \tag{3}$$

where $H_{\rm eff}^{\rm SM}$ includes only the SM box diagrams, while $H_{\rm eff}^{\rm full}$ includes also the NP contributions. In the absence of NP, $C_{B_q} = 1$ and $\phi_{B_q} = 0$. The experimental quantities determined from the $B_q^0 - \bar{B}_q^0$ mixings are related to their SM counterparts and the NP parameters by the following relations:

$$\Delta m_q^{\rm exp} = C_{B_q} \Delta m_q^{\rm SM}\,,\ \beta^{\rm exp} = \beta^{\rm SM} + \phi_{B_d}\,,\ \alpha^{\rm exp} = \alpha^{\rm SM} - \phi_{B_d}\,,\ \beta_s^{\rm exp} = \beta_s^{\rm SM} - \phi_{B_s} \tag{4}$$

For the $K^0 - \bar{K}^0$ mixing is instead convenient to introduce a single parameter:

$$C_{\varepsilon_K} = \frac{{\rm Im}[\langle K^0 | H_{\rm eff}^{\rm full} | \bar{K}^0 \rangle]}{{\rm Im}[\langle K^0 | H_{\rm eff}^{\rm SM} | \bar{K}^0 \rangle]}\,. \tag{5}$$

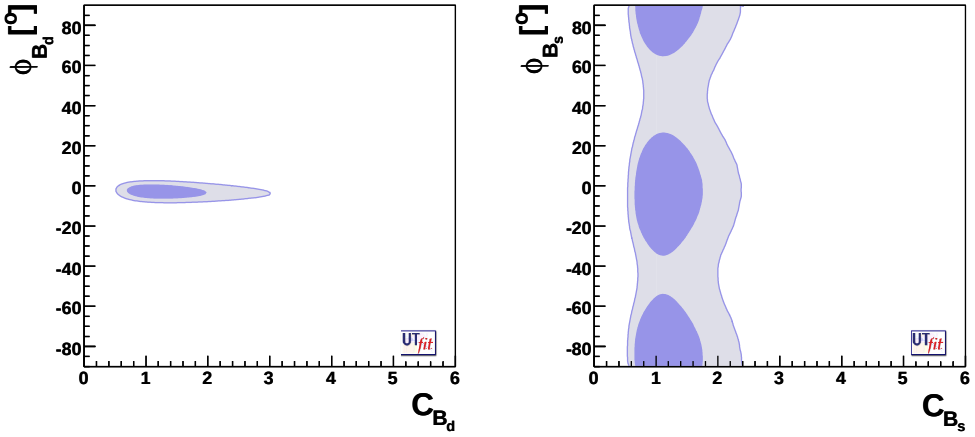

FIGURE 4. Constraints on the $C_{B_q} - \phi_{B_q}$ planes, from the NP generalized UT fit: 68% and 95% confidence regions.

TABLE 3. Determination of UT and NP parameters from the NP generalized fit.

Parameter	Output	Parameter	Output
C_{B_d}	1.25 ± 0.43	$\phi_{B_d}[^\circ]$	-2.9 ± 2.0
C_{B_s}	1.13 ± 0.35	$\phi_{B_s}[^\circ]$	$(-3 \pm 19) \cup (94 \pm 19)$
C_{ε_K}	0.92 ± 0.16		
$\overline{\rho}$	0.20 ± 0.06	$\overline{\eta}$	0.36 ± 0.04
$\alpha[^\circ]$	93 ± 9	$\beta[^\circ]$	24 ± 2
$\gamma[^\circ]$	62 ± 9	$\mathrm{Im}\lambda_t[10^{-5}]$	14.6 ± 1.4
$V_{ub}[10^{-3}]$	4.01 ± 0.25	$V_{cb}[10^{-2}]$	4.15 ± 0.07
$V_{td}[10^{-3}]$	8.3 ± 0.6	$\lvert V_{td}/V_{ts}\rvert$	0.203 ± 0.015
R_b	0.42 ± 0.03	R_t	0.89 ± 0.06
$\sin 2\beta$	0.75 ± 0.04	$\sin 2\beta_s$	0.039 ± 0.004

which implies the following relation for the measured value of ε_K:

$$\varepsilon_K^{\mathrm{exp}} = C_{\varepsilon_K}\, \varepsilon_K^{\mathrm{SM}} \tag{6}$$

In fact, Δm_K is not considered because the long distance effects are not well under control. With these definitions, NP effects which enter the present analysis are parameterized in terms of 5 real quantities: C_{B_d}, ϕ_{B_d}, C_{B_s}, ϕ_{B_s} and C_{ε_K}.

The results of the fit are summarized in Tab. 3. The bounds on the two ϕ_B vs C_B planes are given in Fig. 4. The distributions for C_{B_q}, ϕ_{B_q} and C_{ε_K} are shown in Fig. 5, and in the same figure also the fit result in the $\bar{\rho} - \bar{\eta}$ plane is depicted. We see that the *non-standard* solution for the UT with its vertex in the third quadrant, which was present in

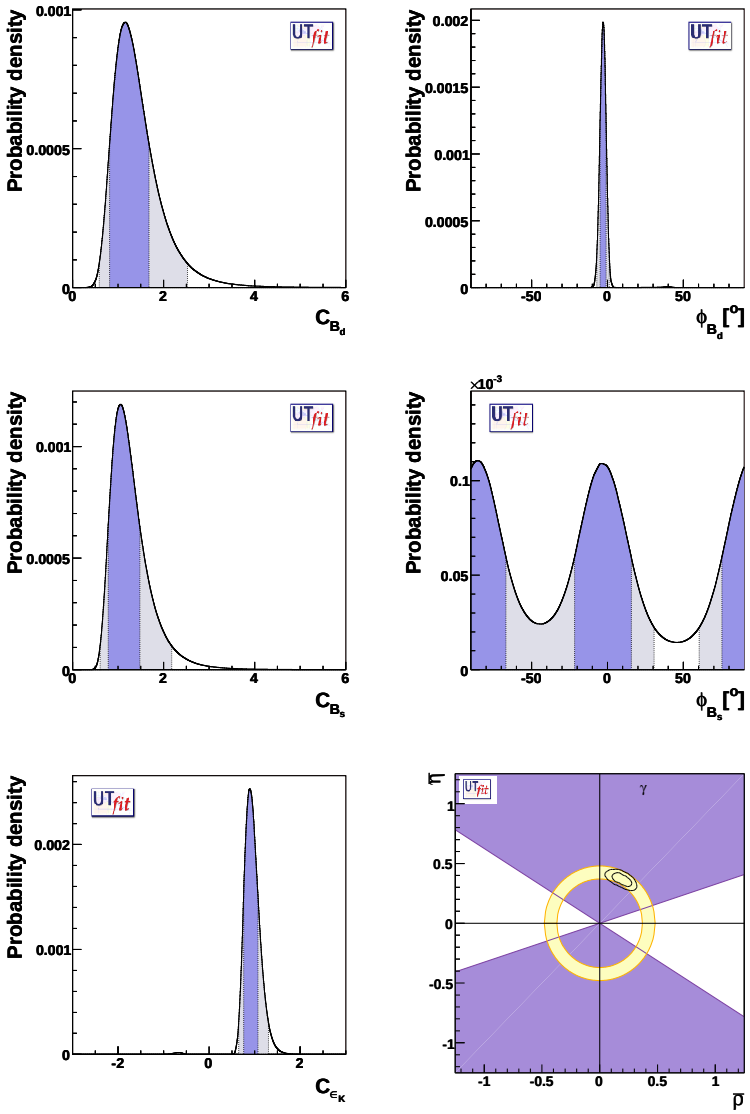

FIGURE 5. Constraints on ϕ_{B_q}, C_{B_q} and C_{ε_K} coming from the NP generalized analysis. The bottom-right plot shows instead the 68% and 95% confidence regions in the $\bar{\rho} - \bar{\eta}$ plane as resulting from the NP generalized fit, superimposed to the 95% confidence regions determined by the $|V_{ub}|/|V_{cb}|$ and γ constraints only.

a previous analysis [2], is now absent thanks to the improved value of $A_{\rm SL}$ by the BaBar Collaboration and to the measurement of $A_{\rm CH}$ by the D0 Collaboration. Furthermore, the measurement of Δm_s strongly constrains C_{B_s}, so that C_{B_s} is already known better than C_{B_d}. Finally, A_{CH} and $\Delta\Gamma_s$ provide the first relevant constraints on ϕ_{B_s}.

UNIVERSAL UNITARITY TRIANGLE ANALYSIS

In the context of MFV extensions of the SM, it is possible to use the so called UUT construction in order to determine the parameters of the CKM matrix independently of NP effects. To this end one has to use all the constraints from tree-level processes and from the angle measurements, as well as the $\Delta m_d/\Delta m_s$ ratio, which in MFV scenarios are NP-free. Instead, ε_K, Δm_d and Δm_s may receive NP contributions, because of the shifts δS_0^K and δS_0^B of the Inami-Lim functions in the K-$\bar{K}$ and $B_{d,s}$-$\bar{B}_{d,s}$ mixings. With only one Higgs doublet or at small $\tan\beta$ these two contributions are forced to be equal. Instead, for large $\tan\beta$, the two quantities are in general different. In both cases, one can use the output of the UUT given in Tab. 4 and in Fig. 6 to constrain $\delta S_0^{K,B}$. We get $\delta S_0 = \delta S_0^K = \delta S_0^B = -0.12 \pm 0.32$ for small $\tan\beta$, while for large $\tan\beta$ we obtain $\delta S_0^B = 0.26 \pm 0.72$ and $\delta S_0^K = -0.18 \pm 0.38$. The output distributions for δS_0^B and δS_0^K are also given in Fig. 6. Using the procedure detailed in [13], these bounds can be translated into lower bounds on the MFV scale Λ:

$$\begin{aligned} \Lambda &> 5.9 \text{ TeV } @95\% \text{ Prob. for small } \tan\beta \\ \Lambda &> 5.4 \text{ TeV } @95\% \text{ Prob. for large } \tan\beta \end{aligned} \tag{7}$$

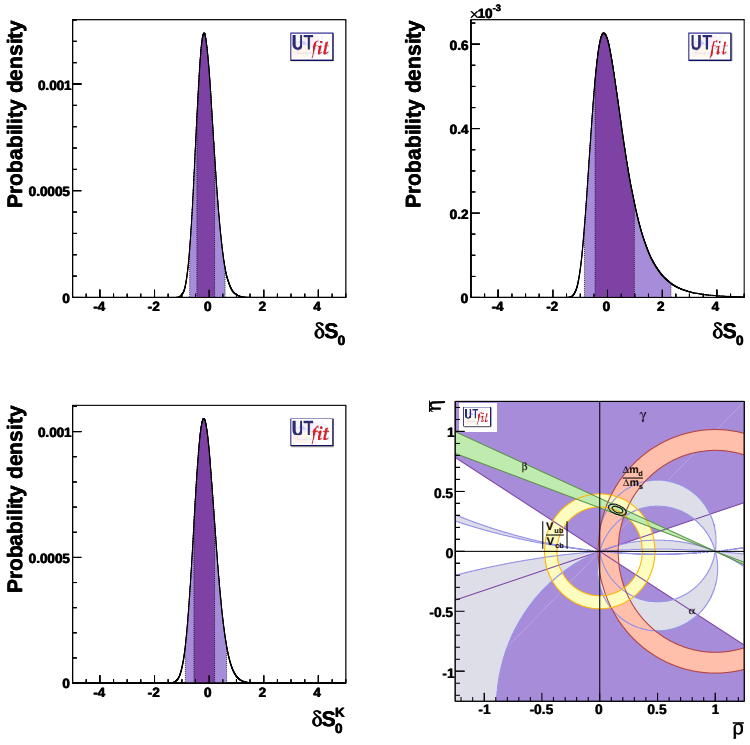

FIGURE 6. P.d.f. of δS_0, δS_0^B and δS_0^K (see the text for details). Bottom-right: Determination of $\bar{\rho}$ and $\bar{\eta}$ from the constraints on α, β, γ, $|V_{ub}/V_{cb}|$, and $\Delta m_d/\Delta m_s$ (UUT fit).

TABLE 4. Determination of UUT parameters from the constraints on α, β, γ, $|V_{ub}/V_{cb}|$, and $\Delta m_d/\Delta m_s$ (UUT fit).

Parameter	Output	Parameter	Output
$\overline{\rho}$	0.154 ± 0.032	$\overline{\eta}$	0.347 ± 0.018
$\alpha[^\circ]$	91 ± 5	$\beta[^\circ]$	22.2 ± 0.9
$\gamma[^\circ]$	66 ± 5	$\sin 2\beta_s$	0.037 ± 0.002

CONCLUSIONS

In this paper we have presented an updated analysis of the UT in the SM, using all the relevant measurements available from the B factories and the Tevatron, in particular the recent measurement of δm_s from CDF.

Then, we have performed a model-independent analysis of the UT in general extensions of the SM with loop-mediated contributions to FCNC processes. We have shown how the great number of measurements nowadays available allow for a simultaneous determination of the CKM parameters, together with the NP contributions to $|\Delta F| = 2$ processes in the K^0, B^0 and B_s^0 sectors.

Finally, we have analyzed in detail the UUT, showing that it is possible to constrain the additional NP parameters very accurately. In this way, we have been able to probe the NP scale in MFV scenarios in the large and small $\tan\beta$ limits up to about 5-6 TeV, to be compared with the SM reference scale of 2.4 TeV.

REFERENCES

1. M. Bona *et al.* [UTfit Collaboration], JHEP **0507**, 028 (2005) [arXiv:hep-ph/0501199].
2. M. Bona *et al.* [UTfit Collaboration], JHEP **0603**, 080 (2006) [arXiv:hep-ph/0509219].
3. M. Bona *et al.* [UTfit Collaboration], arXiv:hep-ph/0606167.
4. M. Bona *et al.* [UTfit Collaboration], arXiv:hep-ph/0605213.
5. M. Ciuchini *et al.*, JHEP **0107** (2001) 013 [arXiv:hep-ph/0012308].
6. [CDF - Run II Collaboration], Phys. Rev. Lett. **97** (2006) 062003 [arXiv:hep-ex/0606027].
7. A. J. Buras *et al.*, Phys. Lett. B **500**, 161 (2001) [arXiv:hep-ph/0007085].
8. E. Gabrielli and G. F. Giudice, Nucl. Phys. B **433**, 3 (1995) [Erratum-ibid. B **507**, 549 (1997)] [arXiv:hep-lat/9407029];
9. M. Misiak, S. Pokorski and J. Rosiek, Adv. Ser. Direct. High Energy Phys. **15**, 795 (1998) [arXiv:hep-ph/9703442];
10. M. Ciuchini *et al.*, Nucl. Phys. B **534**, 3 (1998) [arXiv:hep-ph/9806308];
11. C. Bobeth *et al.*, Nucl. Phys. B **726**, 252 (2005) [arXiv:hep-ph/0505110].
12. M. Blanke *et al.*, arXiv:hep-ph/0604057.
13. G. D'Ambrosio *et al.*, Nucl. Phys. B **645**, 155 (2002) [arXiv:hep-ph/0207036].
14. G. Isidori and P. Paradisi, arXiv:hep-ph/0605012.
15. `http://www-d0.fnal.gov/Run2Physics/WWW/results/prelim/B/B29/B29.pdf`
16. J. M. Soares and L. Wolfenstein, Phys. Rev. D **47**, 1021 (1993);
17. N. G. Deshpande, B. Dutta and S. Oh, Phys. Rev. Lett. **77**, 4499 (1996) [arXiv:hep-ph/9608231];
18. J. P. Silva and L. Wolfenstein, Phys. Rev. D **55**, 5331 (1997) [arXiv:hep-ph/9610208];
19. A. G. Cohen *et al.*, Phys. Rev. Lett. **78**, 2300 (1997) [arXiv:hep-ph/9610252].
20. Y. Grossman, Y. Nir and M. P. Worah, Phys. Lett. B **407**, 307 (1997) [arXiv:hep-ph/9704287].